Published in final edited form as:
J Orthop Res. 2010 December ; 28(12): 1554–1561. doi:10.1002/jor.21187.

Effect of a Focal Articular Defect on Cartilage Deformation during Patello-Femoral Articulation

Benjamin L. Wong, Ph.D.[1] and **Robert L. Sah, M.D., Sc.D.**[1,¥]
[1]Department of Bioengineering, University of California–San Diego, La Jolla, CA.

Abstract

The objective of this study was to determine cartilage strains near, and in apposition to, a focal defect during patello-femoral articulation. Bovine osteochondral blocks from the trochlea (TRO) and patella (PAT) were apposed, compressed 12%, and subjected to sliding under video microscopy. Samples, lubricated with synovial fluid, were tested intact and then with a full-thickness defect in PAT cartilage. Shear (E_{xz}), axial (E_{zz}), and lateral (E_{xx}) strains were determined locally for TRO and PAT cartilage. For articulation with a focal defect, the strain amplitudes of PAT cartilage near the surface were ~2–8× lower in E_{xz} and ~1.4× higher in $-E_{zz}$ than intact PAT cartilage. At 20% depth, E_{xz} and E_{xx} for PAT cartilage with a focal defect were ~2× and ~10–25× higher than intact PAT, respectively. For TRO articulating against a focal defect, E_{xz} and $-E_{zz}$ near the surface and at 20% depth were ~2–4× lower than that for articulation against intact cartilage. The results elucidate dramatic region-specific changes in strain due to lateral motion. In these regions, such altered cartilage mechanics during knee movement may cause focal defects to extend by induction of damaging levels of strain to bordering regions of cartilage.

Keywords

focal defect; articulation; biomechanics; deformation; cartilage strains

INTRODUCTION

Focal articular defects are prevalent in symptomatic knees and are associated with progressive cartilage degeneration. In patients evaluated arthroscopically, focal defects were found in 20–60% of all symptomatic knees, occurring most frequently in the medial condyle and patella, both of which are load-bearing regions (Figure 1).[1–4] Such, focal defects typically ranged from 0.5 to 4cm^2 in area with an average area of 2.1cm^2, and extended beyond half the cartilage thickness in depth in 50% of all visualized articular defects.[1] With continued joint loading and time, untreated defects enlarge,[5] are associated with cartilage volume loss,[6] and exhibit histopathological signs of cartilage degeneration adjacent to the focal defect.[7,8] While such findings suggest that the presence of a focal defect predisposes joints to secondary osteoarthritis, the mechanism by which it causes cartilage within the proximity of a focal defect to degenerate remains to be elucidated.

The effect of a focal defect on cartilage deformation has been examined during axially-directed loading. Under such axial compression alone, contact stress and stress gradients are elevated in areas of cartilage near the edges of a focal defect.[9,10] As a result, macroscopic

¥Address correspondence and reprint requests to Robert L. Sah, MD, ScD, Department of Bioengineering, Mail Code 0412, University of California–San Diego, 9500 Gilman Drive, La Jolla, CA 92093-0412. Tel: (858) 534-0821. Fax: (858) 822-1614. rsah@ucsd.edu.

tissue deformation[11] and local strains[12] are increased markedly in these regions. Elevated strains may reach levels that induce cell death[13] and matrix damage,[14] and thus, the elevated strains resulting from a focal defect may become injurious to cartilage and induce degeneration. Such tissue deformation may be altered by or accentuated with the addition of lateral motion superimposed on compression, as both occur in load-bearing regions of cartilage during joint movement.

During knee movement, articular surfaces contact, compress, and articulate against each other. Within the patellofemoral groove of the knee, patellar cartilage contacts and slides against trochlear cartilage during normal joint movement and loading (Figure 2A). Under applied compressive loads of ~1.5× the body weight, patellofemoral cartilage compresses ~10% of its overall thickness *in vitro* following 14 minutes of static loading,[15] and following knee bending, patellar cartilage alone compresses about ~5–10% overall *in vivo.*[16] Collectively, such results provide physiologic mechanical parameters for the *in vitro* testing of patello-femoral articulation.

Recently, local and overall deformation of cartilage during compression and cartilage articulation[17] were determined using video microscopy[18] and image correlation to track the displacement of fiduciary markers.[19,20] Such a test configuration can be applied to study contact of patellar and trochlear cartilage surfaces,[21,22] to examine the effects of a focal articular defect on the deformation cartilage near, and in apposition to, the proximal defect edge that experiences oncoming forward motion of the apposing surface during compression and lateral displacement (Figure 2).

Therefore, the hypothesis of this study was that during patellofemoral cartilage articulation, the cartilage deformation of the patella and trochlea are markedly altered with the presence of a focal articular defect. The specific objective of this study was to determine the effects of a focal articular defect, created in the patellar tissue, on the local and overall strains of the patellar and trochlear cartilage during compression and sliding motion.

MATERIALS AND METHODS

Sample Isolation and Preparation

Osteochondral cores with macroscopically normal cartilage were harvested from the trochlea (TRO) and patella (PAT) of four adult bovine animals (1–2yrs). Using a low speed drill press with custom stainless steel coring bits, a 10mm diameter osteochondral core was isolated from both the TRO and PAT of each joint in a manner similar to that described previously.[23] The TRO and PAT cores were then trimmed to each yield one ~rectangular block for biomechanical testing.[17] Each rectangular block had a cartilage surface area of ~3×10mm^2 and a total thickness of ~1cm (Figure 2A). Each sample consisted of one TRO and one PAT block from the same knee, and was stored in phosphate buffered saline (PBS) containing proteinase inhibitors (PI) until testing.

Prior to mechanical testing, samples were stained for ~2–4h at 4°C in PBS+PI and propidium iodide (20μg/ml) to fluorescently highlight cell nuclei. Blocks were then bathed in normal bovine synovial fluid (SF) containing PI and propidium iodide (20μg/ml) at 4°C for 12–16h to lubricate surfaces. The SF was pooled from adult bovine knees, stored at −80°C, and characterized previously for boundary lubrication properties and lubricant molecules levels.[23]

Experimental Design

To characterize the effect of a focal defect on cartilage deformation during articulation, samples were mechanically tested, first intact and then with a focal defect. In between tests,

samples were rinsed, allowed to reswell, and incubated for ~2–4h in PBS+PI and then in SF +PI for an additional 12–16h at 4°C. Following the mechanical testing of intact samples and reincubation, a full thickness, 3mm wide focal articular defect was created in the center of the PAT cartilage (Figure 2A) as described previously.[12] The width of the focal defect was chosen so to be wide relative to the articulation distance (described below) in order to focus on the initial stages of articulation.

Micro-scale Shear Testing

Samples were shear tested under video microscopy essentially as described previously.[17] Briefly, each TRO and PAT pair was secured in a custom bi-axial loading chamber mounted onto an epi-fluorescence microscope for digital video imaging (Figure 2B).[18] The chamber secured the PAT block at the bone and allowed in-plane movement of the apposing mobile TRO block with orthogonally positioned plungers. Subsequently, an axial displacement was applied (~40μm/s) to induce 12% compression ($1-\Lambda_z$, where Λ_z is the stretch ratio[24]) of the overall cartilage thickness (Figure 2B). Samples were then allowed to stress relax for 1h, determined to be sufficient to reach an approximate equilibrium stress for the current sample geometries.[17] Cartilage deformation was then captured during lateral motion separately in the TRO and PAT cartilage following axial compression. Three sets of applied lateral displacements (Δx), each consisting of +1mm and then −1mm (returning to initial position) were applied at 100μm/s to the bone portion of the TRO block (Figure 2B). The first set, was for preconditioning[23], while the second and third set were recorded for the PAT and TRO blocks for analysis, respectively. Deformation during patello-femoral cartilage articulation was captured with sequential fluorescence images taken at ~25μm increments of lateral displacement.

Data Collection and Calculations

Acquired images were analyzed as described previously[17,20] to determine the depth-varying and overall deformation and strain in cartilage. Evenly-distributed cell nuclei (~250 cells/mm^2) were tracked during lateral motion to determine the displacements of uniformly-spaced (10 pixel) mesh points in local regions. Subsequently, Lagrangian shear (E_{xz}), axial (E_{zz}), and lateral (E_{xx}) strains were determined relative to the unloaded state[24], when articular surfaces were sliding ($\Delta x = 0.8$mm) and strains had become steady. Local strains were determined by averaging depth-wise and at various lateral distances from the defect edge. First, sample thickness was normalized and divided into 8 intervals, with 4 intervals being 0.083 times the normalized thickness near the articular surface (i.e. 0 to 0.333) and 0.167 times for the remaining tissue depth (i.e. 0.333 to 1). To reduce noise and consolidate data, PAT cartilage strains near the proximal defect edge, which experiences forward lateral motion, were averaged depth-wise for lateral regions (~0.2mm × full cartilage thickness) at (EDGE), ~0.4mm (MID) and ~0.8mm (FAR) away from the defect edge to yield a depth-profile at varying lateral distances (Figure 2C). For TRO cartilage in direct apposition to the focal defect prior to lateral motion, strains following lateral articulation were averaged depth-wise in lateral regions (~0.15mm × full cartilage thickness) at (EDGE), ~0.3mm (MID), and ~0.5mm (FAR) away from the defect edge. For intact tissue, strains in corresponding lateral regions were determined similarly. Overall strain values were determined as the mean of all local values.

Statistical Analysis

Data are reported as mean ± standard error of the mean (SEM). Repeated measures ANOVA was used to determine the effects of a focal defect (intact versus defect), tissue depth, and lateral location from the defect edge (EDGE, MID, FAR) on local and overall strains. Differences between defect and intact samples at the various lateral locations were assessed by planned pair-wise comparisons.

RESULTS

Qualitatively, the deformations of intact PAT and TRO cartilage were similar, being depth-varying during axial compression as well as during lateral motion. Cartilage thickness was similar between intact samples, being 1.97 ± 0.13mm and 1.93 ± 0.14mm for PAT and TRO tissue, respectively. Under compression, axial deformation of intact PAT and TRO cartilage were similarly depth-varying, being highest near the surface and lowest near the tidemark. Also during compression, shear and lateral deformation were low (<0.01) for both PAT and TRO cartilage. During lateral motion, shear deformation was depth-varying for both intact PAT and TRO cartilage, being highest at the surface and decreasing monotonically with tissue depth. In contrast, axial and lateral deformation appeared to not be affected by lateral motion.

Qualitatively, creation of a focal defect in the PAT cartilage led to alterations in the gross deformation of TRO and PAT cartilage during axial compression and lateral motion. Under compression, TRO cartilage directly in apposition to the focal defect partially filled the empty defect region (Figure 3B,E,H). Consequently, PAT cartilage near the proximal defect edge bulged into the defect region (expanding laterally outward just beneath the surface) and compressed further. With lateral motion, the TRO cartilage partially filling the defect plowed over and further compressed the proximal defect edge, while becoming compressed itself as it slid over the PAT surface (see Video Supplements).

Patellar Cartilage Deformation

Shear Strain (E_{xz})—Following compression and lateral articulation, E_{xz} of PAT cartilage was depth-varying ($p<0.001$), both without (i.e. intact) and with a focal defect (Figure 3A,B), and markedly different due to a defect ($p<0.05$). With lateral articulation, E_{xz} of intact, cartilage did not vary with lateral location ($p=0.6$) and decreased slightly and monotonically from ~0.08 near the surface to relatively low magnitudes (≤0.01) near the tidemark (Figure 3C). With lateral articulation and a focal defect, cartilage E_{xz} was also depth-varying; however, strains peaked at ~20% tissue depth and became a minimum at ~40% depth for all lateral locations (Figure 3C). Near the surface, E_{xz} of cartilage with a defect tended ($p=0.07$) to be ~2–8× lower than that for intact (Figure 4A). With increasing lateral distance from the defect edge, surface E_{xz} decreased from ~0.05 to 0.01 for cartilage with a defect ($p<0.01$), while remained constant for intact samples. At 20% tissue depth, E_{xz} was ~2× higher for cartilage with a defect than intact samples ($p<0.01$), being significantly higher at EDGE ($p<0.05$) and MID ($p<0.01$) regions (Figure 4B). Overall, E_{xz} of cartilage with a defect was 4–5× times lower ($p<0.05$) than that for intact cartilage and did not vary markedly with lateral location ($p=0.15$) (Figure 4C). Qualitatively, the results indicate that PAT cartilage near the proximal defect edge strains less near the surface, and more at 20% depth, in shear than intact cartilage during lateral articulation.

Axial Strain (E_{zz})—Compressive strain ($-E_{zz}$) of PAT cartilage decreased significantly with depth from the articular surface ($p<0.001$) for both intact and defect samples (Figure 3D–F), and was markedly higher for cartilage with a focal defect ($p<0.05$). With increasing tissue depth, $-E_{zz}$ decreased significantly from 0.32 and 0.43 near the surface to ~0.04 near the tidemark for both intact and defect samples, respectively (Figure 3F). Near the articular surface (Figure 4D) and overall (Figure 4F), $-E_{zz}$ of cartilage with a defect was ~1.4× higher ($p<0.05$) than that of intact cartilage. At 20% tissue depth, $-E_{zz}$ of cartilage with a defect tended to be ~1.8× greater ($p=0.2$) than that in intact cartilage (Figure 4E). Cartilage $-E_{zz}$ with and without a defect did not vary with lateral location near the surface ($p=0.25$) and at 20% depth ($p=0.7$), being similar to overall $-E_{zz}$ of intact cartilage (Figure 4D–F). However, overall $-E_{zz}$ of cartilage with a defect decreased with increasing lateral distance from the

defect edge ($p<0.01$). Thus, when TRO cartilage filling the focal defect slides over the proximal defect edge, PAT cartilage near a focal defect compresses more than intact cartilage near the surface and overall.

Lateral Strain (E_{xx})—With articulation, the resultant E_{xx} for intact cartilage did not vary significantly with tissue depth ($p=0.2$) and lateral location ($p=1.0$) (Figure 3G), while for cartilage with a defect, E_{xx} varied with tissue depth ($p<0.001$) and lateral region ($p<0.01$) (Figure 3H). For all lateral regions, E_{xx} remained negligible (≤0.01) for intact cartilage throughout tissue depth and peaked at ~20% depth for defect samples (Figure 3I). Near the articular surface, E_{xx} for cartilage with a defect were statistically indifferent ($p=0.4$) from that for intact cartilage and did not significantly ($p=0.6$) vary with lateral distance (Figure 4G). At 20% tissue depth (Figure 4H) and overall (Figure 4I), cartilage E_{xx} peaked at a value of ~0.08 and ~0.03, respectively, in the MID region for cartilage with a defect ($p<0.01$) and were significantly higher than E_{xx} for intact cartilage ($p<0.01$). Thus, PAT cartilage expands laterally at 20% tissue depth as it becomes further compressed when TRO cartilage filling the focal defect slides over the defect edge.

Trochlear Cartilage Deformation

During patello-femoral articulation, the depth-variation in strains of TRO cartilage in articulation with an intact and defect-containing PAT surface were similar to that of PAT cartilage (Figure 5), and the effect of a focal defect on TRO cartilage strains were also marked (Figure 6). For TRO cartilage in articulation with an intact PAT surface, E_{xz} and $-E_{zz}$ were highest near the surface and decreased with increasing depth ($p<0.001$), while E_{xx} remained negligible throughout tissue depth ($p=0.6$). All strains did not vary with lateral region for TRO articulation with intact PAT cartilage ($p=0.15$–0.6). For TRO cartilage in articulation with a focal defect, E_{xz} and $-E_{zz}$ were ~2–3× ($p<0.05$, Figure 6A) and ~2–4× ($p<0.01$, Figure 6D), respectively, less near the surface than when in articulation with an intact surface. Furthermore, TRO cartilage compressed laterally in the EDGE region near the surface, and E_{xx} near the surface markedly increased with lateral distance ($p<0.05$), transitioning into lateral tension in the MID and FAR regions (Figure 6G). The effects of tissue depth, lateral region, and a focal defect on TRO strains during lateral articulation are described in further detail in the supplementary data.

DISCUSSION

This study elucidated the deformation of cartilage within the proximity of, and directly in apposition to, a focal articular defect during patello-femoral cartilage articulation. As the TRO surface displaced laterally, the tissue partially filling the focal defect pushed and then plowed over the proximal defect edge. As a result, PAT cartilage proximal to the defect sheared markedly less (~70–700%) near the surface and more (~50–60%) at 20% tissue depth than intact cartilage during lateral motion (Figure 7). PAT cartilage near the focal defect also compressed more (30–40%) than intact cartilage, and expanded laterally ~10–25× more at 20% tissue depth than intact cartilage as TRO cartilage translated laterally over the proximal defect edge. For regions directly in apposition to the focal defect, TRO cartilage sheared and compressed less (~50–70%) than when it slid over intact cartilage. As the TRO surface plowed over the proximal defect edge, TRO cartilage near the surface also compressed laterally at the EDGE region, while expanded laterally at MID and FAR regions. Collectively, the current results indicate that with articulation, the tissue deformation of both the cartilage adjacent to, and in apposition to, a focal defect are altered drastically by the presence of a focal defect, extending the findings of strain analysis of cartilage when compressed.[12]

While patellar cartilage was analyzed up to the articular surface, the region very close to the trochlear surface (~10% of tissue depth), which partially filled the defect, was not analyzed because during lateral motion, tissue compression was so extensive in that region that cell nuclei coalesced and could not be discriminated and tracked. However, regions directly in apposition of the defect edge (EDGE) prior to lateral motion were tracked appropriately near the surface. Thus, strains in other lateral regions (MID, FAR) of the trochlear cartilage may be somewhat (~10–15%) underestimated and may be more similar to the values of the EDGE lateral region.

The dramatic elevation in cartilage strains near a focal defect during lateral articulation may be related to, and contribute to, the progressive tissue degeneration associated with focal defects. With joint loading and time, increased fibrillation and decreased matrix staining were noted in regions adjacent to a focal defect in animal models.[7,8] Also, untreated defects in human knee joints have been shown to enlarge[5] and be associated with cartilage volume loss.[6] Markedly elevated strains likely make cartilage susceptible to damage in these regions, via cell death[13] and matrix damage,[14] which can be induced by high magnitudes of compression. With repeated loading during joint movement, the increased E_{xz} and E_{xx} at 20% tissue depth, as well as the elevated $-E_{zz}$ near the surface, may all contribute to inducing, and be related to, the indicators of tissue degeneration characterized previously near the focal defect edge. Thus, focal defects may enlarge due to articulation-induced strain that is damaging to the bordering regions of cartilage.

For cartilage in direct apposition to focal defects, the reduction in localized strains during lateral articulation may be related to the low incidences of two focal defects being in direct apposition (i.e. “kissing lesions”). Focal defects found on both apposing cartilage surfaces were found in only ~2% of the symptomatic knees arthroscopically diagnosed with focal defects.[3] The low frequency of kissing lesions may be attributed the reduction in E_{xz} and $-E_{zz}$ of cartilage when in articulation with a focal defect. Since strain magnitudes are lowered, a chondral defect may unlikely develop from a pre-existing focal defect on the opposing surface. Instead, kissing lesions may form with the defects being initiated concurrently at the time of injury or with one lesion enlarging big enough to become full-thickness in depth and cause the apposing chondral surface to be in articulation against the subchondral bone, inducing abrasive wear.

The present study suggests that focal articular defects drastically alter cartilage deformation of both apposing cartilage surfaces not only during axial loading, but also during lateral articulation. Focal defects, which a majority (~61%) has been associated with acute injury or trauma,[1] markedly alter the mechanical environment of cartilage, and the resulting abnormal strains may be injurious to cells and matrix. Mechanically induced cell death and tissue loss reduce cell population and likely compromise the overall biosynthetic response of the tissue.[25] While for the remaining viable cells that may continue to experience injurious levels of strain, their metabolic activities are markedly altered.[13,14] As a result, tissue repair and remodeling responses are likely compromised, eventually leading to changes in cartilage structure by degeneration and wear. Thus, the changes in cartilage deformation associated with focal effects during both axial loading and lateral articulation may contribute to the enlargement of focal defects and predispose joints to secondary osteoarthritis.

Supplementary Material

Refer to Web version on PubMed Central for supplementary material.

Acknowledgments

This work was supported by NIH and the Howard Hughes Medical Institute through the Professors Program to UCSD (for RLS). We thank Chris Kim and Alexander Cigan for assistance with the sample preparations.

REFERENCES

1. Hjelle K, Solheim E, Strand T, Muri R, Brittberg M. Articular cartilage defects in 1,000 knee arthroscopies. Arthroscopy. 2002; 18:730–734. [PubMed: 12209430]
2. Curl WW, Krome J, Gordon ES, Rushing J, Smith BP, Poehling GG. Cartilage injuries: a review of 31,516 knee arthroscopies. Arthroscopy. 1997; 13:456–460. [PubMed: 9276052]
3. Aroen A, Loken S, Heir S, Alvik E, Ekeland A, Granlund OG, Engebretsen L. Articular cartilage lesions in 993 consecutive knee arthroscopies. Am J Sports Med. 2004; 32:211–215. [PubMed: 14754746]
4. Widuchowski W, Widuchowski J, Trzaska T. Articular cartilage defects: study of 25,124 knee arthroscopies. Knee. 2007; 14:177–182. [PubMed: 17428666]
5. Wang Y, Ding C, Wluka AE, Davis S, Ebeling PR, Jones G, Cicuttini FM. Factors affecting progression of knee cartilage defects in normal subjects over 2 years. Rheumatology (Oxford). 2006; 45:79–84. [PubMed: 16188947]
6. Cicuttini F, Ding C, Wluka A, Davis S, Ebeling PR, Jones G. Association of cartilage defects with loss of knee cartilage in healthy, middle-age adults: a prospective study. Arthritis Rheum. 2005; 52:2033–2039. [PubMed: 15986359]
7. Lefkoe TP, Trafton PG, Ehrlich MG, Walsh WR, Dennehy DT, Barrach HJ, Akelman E. An experimental model of femoral condylar defect leading to osteoarthrosis. J Orthop Trauma. 1993; 7:458–467. [PubMed: 8229383]
8. Jackson DW, Lalor PA, Aberman HM, Simon TM. Spontaneous repair of full-thickness defects of articular cartilage in a goat model. A preliminary study. J Bone Joint Surg Am. 2001; 83-A:53–64. [PubMed: 11205859]
9. Brown TD, Pope DF, Hale JE, Buckwalter JA, Brand RA. Effects of osteochondral defect size on cartilage contact stress. J Orthop Res. 1991; 9:559–567. [PubMed: 2045983]
10. Guettler JH, Demetropoulos CK, Yang KH, Jurist KA. Osteochondral defects in the human knee: influence of defect size on cartilage rim stress and load redistribution to surrounding cartilage. Am J Sports Med. 2004; 32:1451–1458. [PubMed: 15310570]
11. Braman JP, Bruckner JD, Clark JM, Norman AG, Chansky HA. Articular cartilage adjacent to experimental defects is subject to atypical strains. Clin Orthop Relat Res. 2005; 430:202–207. [PubMed: 15662325]
12. Gratz KR, Wong BL, Bae WC, Sah RL. The effects of focal articular defects on cartilage contact mechanics. J Orthop Res. 2009; 27:584–592. [PubMed: 18979528]
13. Kurz B, Jin M, Patwari P, Cheng DM, Lark MW, Grodzinsky AJ. Biosynthetic response and mechanical properties of articular cartilage after injurious compression. J Orthop Res. 2001; 19:1140–1146. [PubMed: 11781016]
14. Quinn TM, Allen RG, Schalet BJ, Perumbuli P, Hunziker EB. Matrix and cell injury due to sub-impact loading of adult bovine articular cartilage explants: effects of strain rate and peak stress. J Orthop Res. 2001; 19:242–249. [PubMed: 11347697]
15. Herberhold C, Faber S, Stammberger T, Steinlechner M, Putz R, Englmeier KH, Reiser M, Eckstein F. In situ measurement of articular cartilage deformation in intact femoropatellar joints under static loading. J Biomech. 1999; 32:1287–1295. [PubMed: 10569707]
16. Eckstein F, Lemberger B, Stammberger T, Englmeier KH, Reiser M. Patellar cartilage deformation in vivo after static versus dynamic loading. J Biomech. 2000; 33:819–825. [PubMed: 10831756]
17. Wong BL, Bae WC, Chun J, Gratz KR, Sah RL. Biomechanics of cartilage articulation: effects of lubrication and degeneration on shear deformation. Arthritis Rheum. 2008; 58:2065–2074. [PubMed: 18576324]
18. Schinagl RM, Gurskis D, Chen AC, Sah RL. Depth-dependent confined compression modulus of full-thickness bovine articular cartilage. J Orthop Res. 1997; 15:499–506. [PubMed: 9379258]

19. Wang CC, Deng JM, Ateshian GA, Hung CT. An automated approach for direct measurement of two-dimensional strain distributions within articular cartilage under unconfined compression. J Biomech Eng. 2002; 124:557–567. [PubMed: 12405599]

20. Gratz KR, Sah RL. Experimental measurement and quantification of frictional contact between biological surfaces experiencing large deformation and slip. J Biomech. 2008; 41:1333–1340. [PubMed: 18329650]

21. Erne OK, Reid JB, Ehmke LW, Sommers MB, Madey SM, Bottlang M. Depth-dependent strain of patellofemoral articular cartilage in unconfined compression. J Biomech. 2005; 38:667–672. [PubMed: 15713286]

22. Guterl CC, Gardner TR, Rajan V, Ahmad CS, Hung CT, Ateshian GA. Two-dimensional strain fields on the cross-section of the human patellofemoral joint under physiological loading. J Biomech. 2009; 42:1275–1281. [PubMed: 19433326]

23. Schmidt TA, Sah RL. Effect of synovial fluid on boundary lubrication of articular cartilage. Osteoarthritis Cartilage. 2007; 15:35–47. [PubMed: 16859933]

24. Fung, YC. A First Course in Continuum Mechanics. Englewood Cliffs: Prentice-Hall; 1977.

25. Hunziker EB, Quinn TM. Surgical removal of articular cartilage leads to loss of chondrocytes from cartilage bordering the wound edge. J Bone Joint Surg Am. 2003; 85-A(Suppl 2):85–92. [PubMed: 12721349]

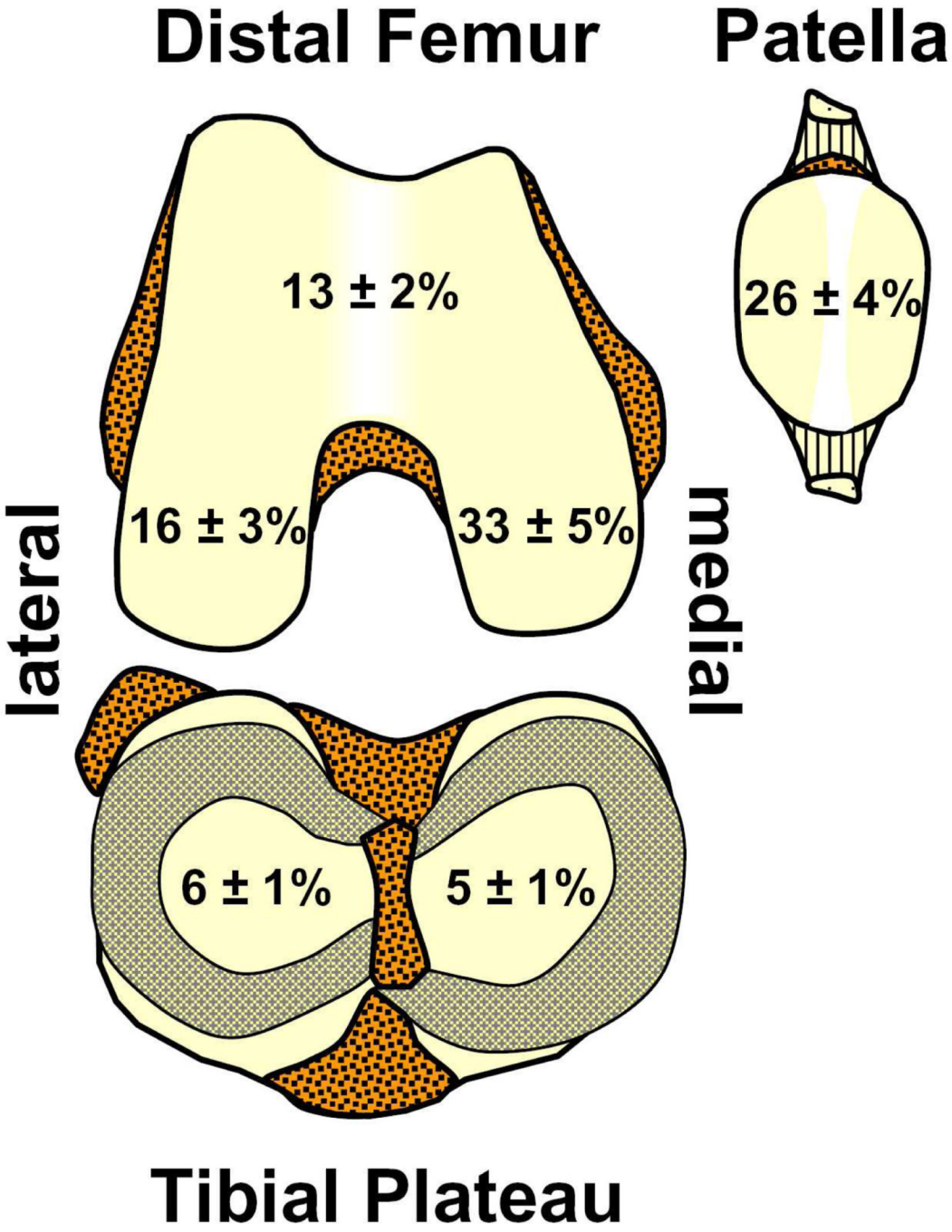

Figure 1.
Anatomical distribution of focal articular defects averaged from four previous arthroscopy studies on the prevalence of cartilage defects in symptomatic knees.[1–4]

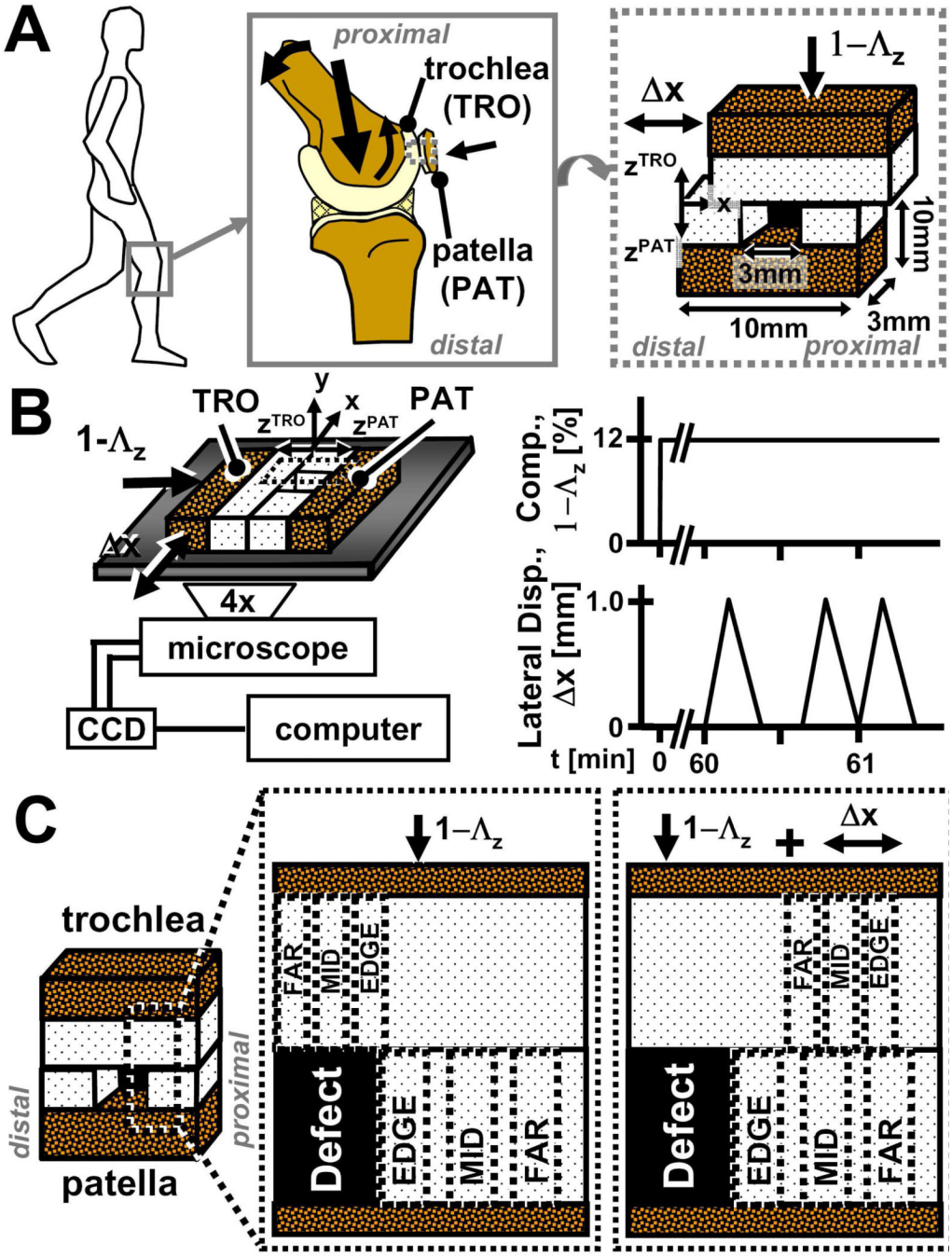

Figure 2.

Schematic of (**A**) knee joint movements at multiple scales, (**B**) experimental setup and loading protocol for micro-shear testing, (**C**) and locations of sub-regions (EDGE, MID, FAR) used for statistical analysis of strains in patella and trochlear cartilage.

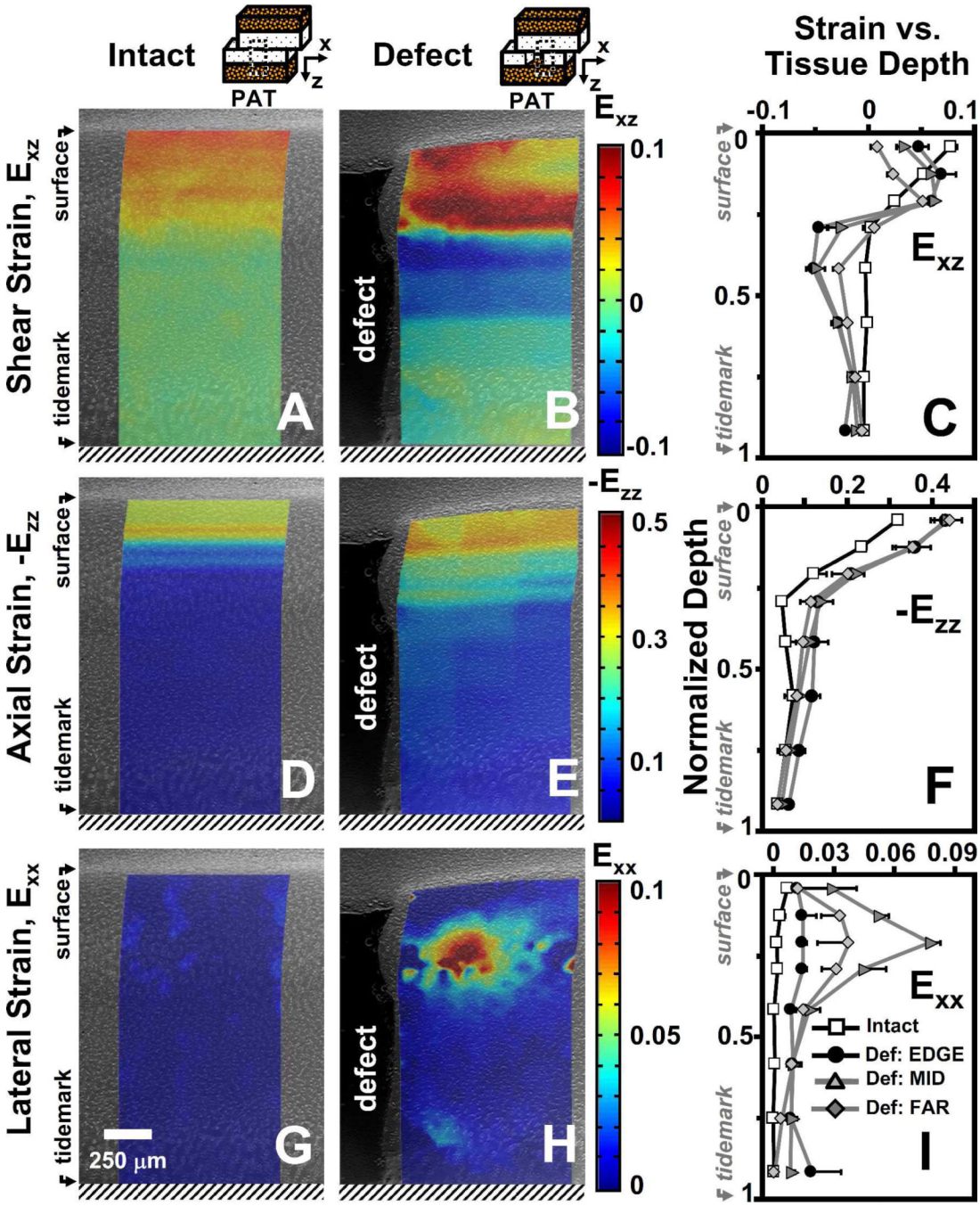

Figure 3.

Representative micrographs of patellar cartilage as (**A,D,G**) intact or (**B,E,H**) with a focal defect with superimposed colormaps of (**A,B**) shear (E_{xz}), (**D,E**) axial ($-E_{zz}$), and (**G,H**) lateral (E_{xx}) strain maps when articulating against trochlear samples after articular surfaces have slid. Strain map boundaries encompass the corresponding deformed states. Local (**C**) shear (E_{xz}), (**F**) axial ($-E_{zz}$), and (**I**) lateral (E_{xx}) strain averaged depth-wise versus normalized tissue depth for patella cartilage as intact or with a focal defect. For samples with a focal defect, strains were also determined as a function of lateral distance from the defect edge (EDGE, MID, FAR). Values are mean ± SEM.

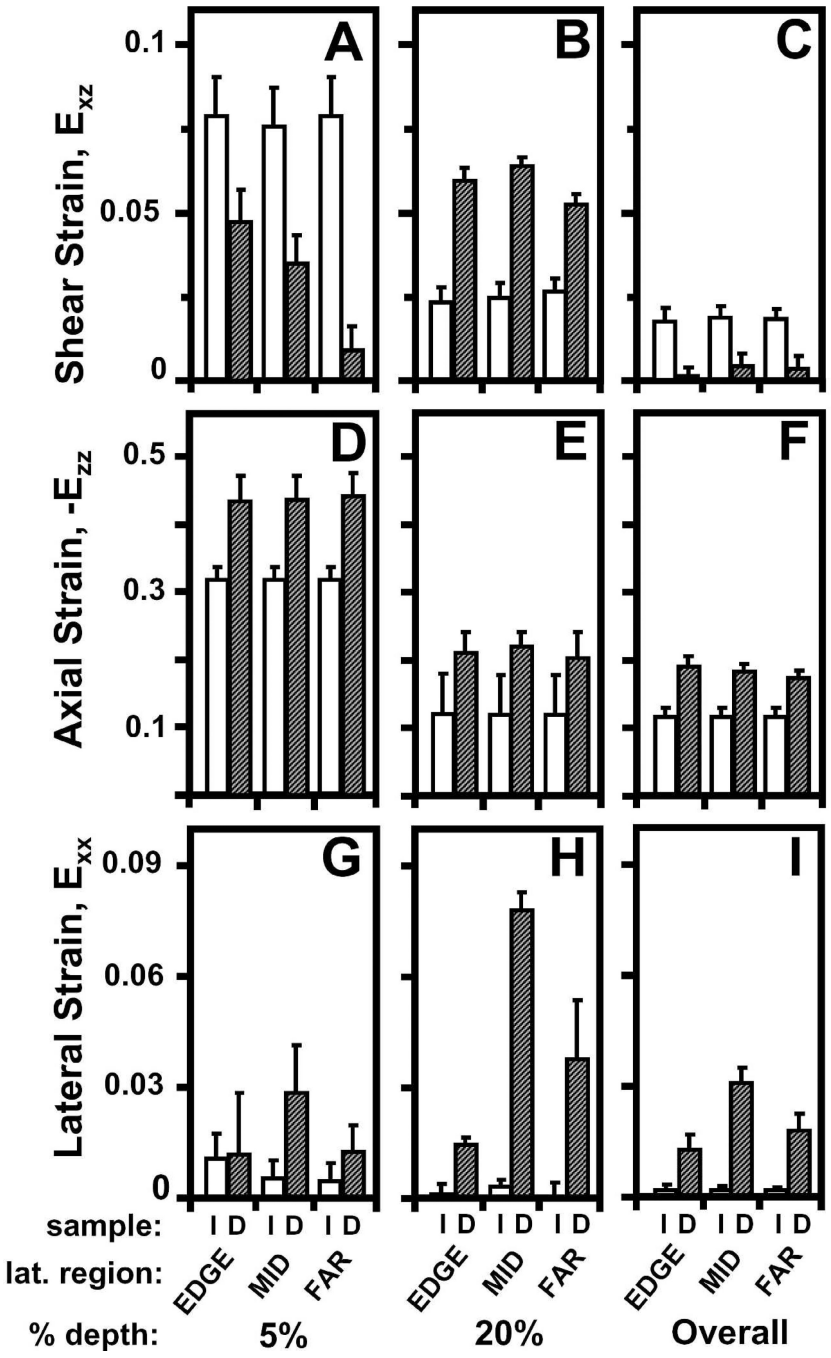

Figure 4.

Effect of a focal defect (intact (I) versus defect (D)) on (**A–C**) shear, (**D–F**) axial, and (**G–I**) lateral strain (**A,D,G**) near the articular surface, (**B,E,H**) at 20% tissue depth, and (**C,F,I**) overall on patellar cartilage during articulation.

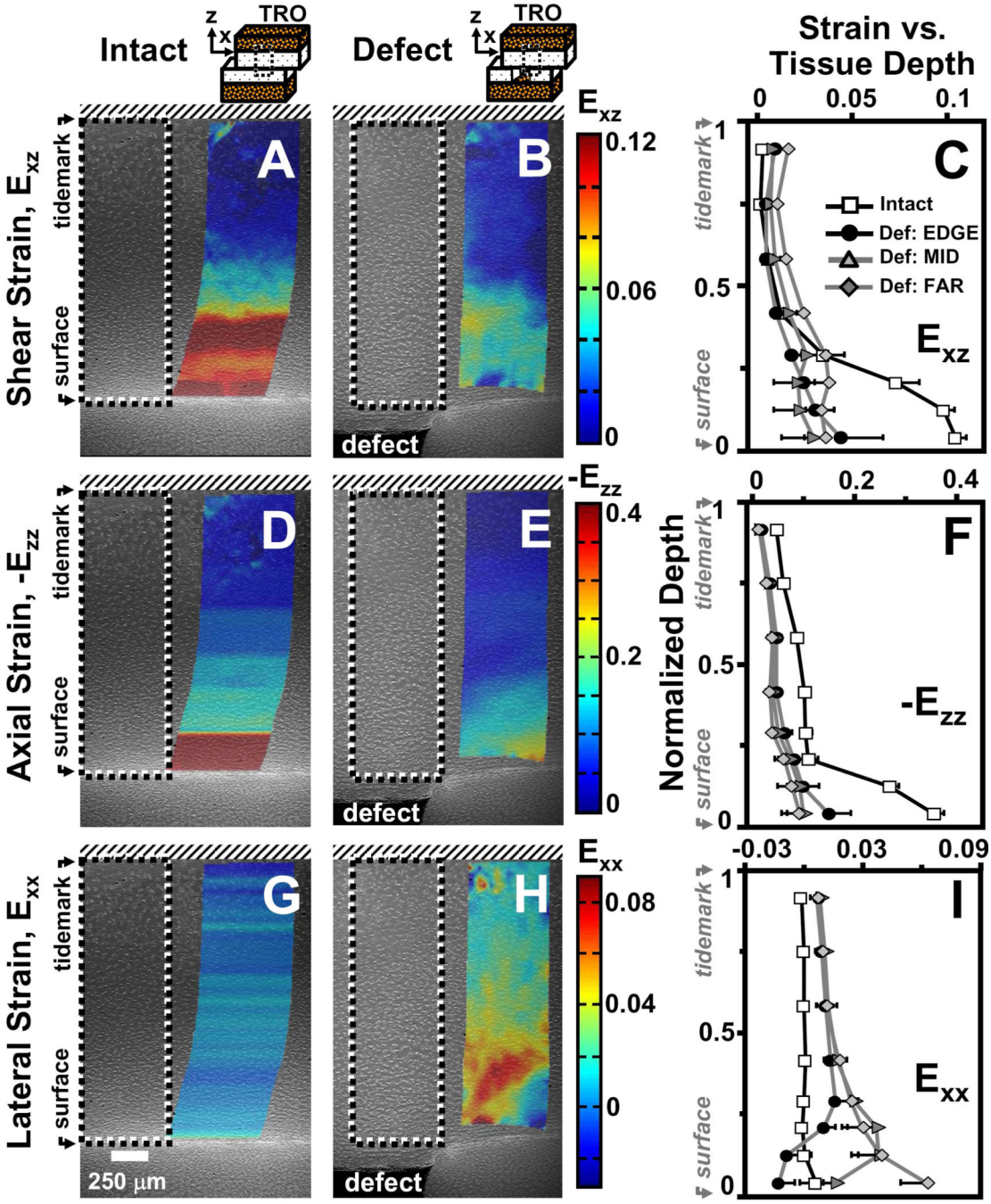

Figure 5.

Representative micrographs of trochlear cartilage with superimposed colormaps of (**A,B**) shear (E_{xz}), (**D,E**) axial ($-E_{zz}$), and (**G,H**) lateral (E_{xx}) strain when in apposition with patellar cartilage as (**A,D,G**) intact or (**B,E,H**) with a focal defect during lateral motion. Dashed lines (– –) encompass the analyzed regions prior to lateral motion, while boundaries of strain maps encompass the corresponding deformed states. Local (**C**) shear (E_{xz}), (**F**) axial ($-E_{zz}$), and (**I**) lateral (E_{xx}) strain averaged depth-wise versus normalized tissue depth for trochlear cartilage, intact or with a focal defect. For samples apposing a focal defect,

strains were also determined as a function of lateral distance from the defect edge (EDGE, MID, FAR). Values are mean ± SEM.

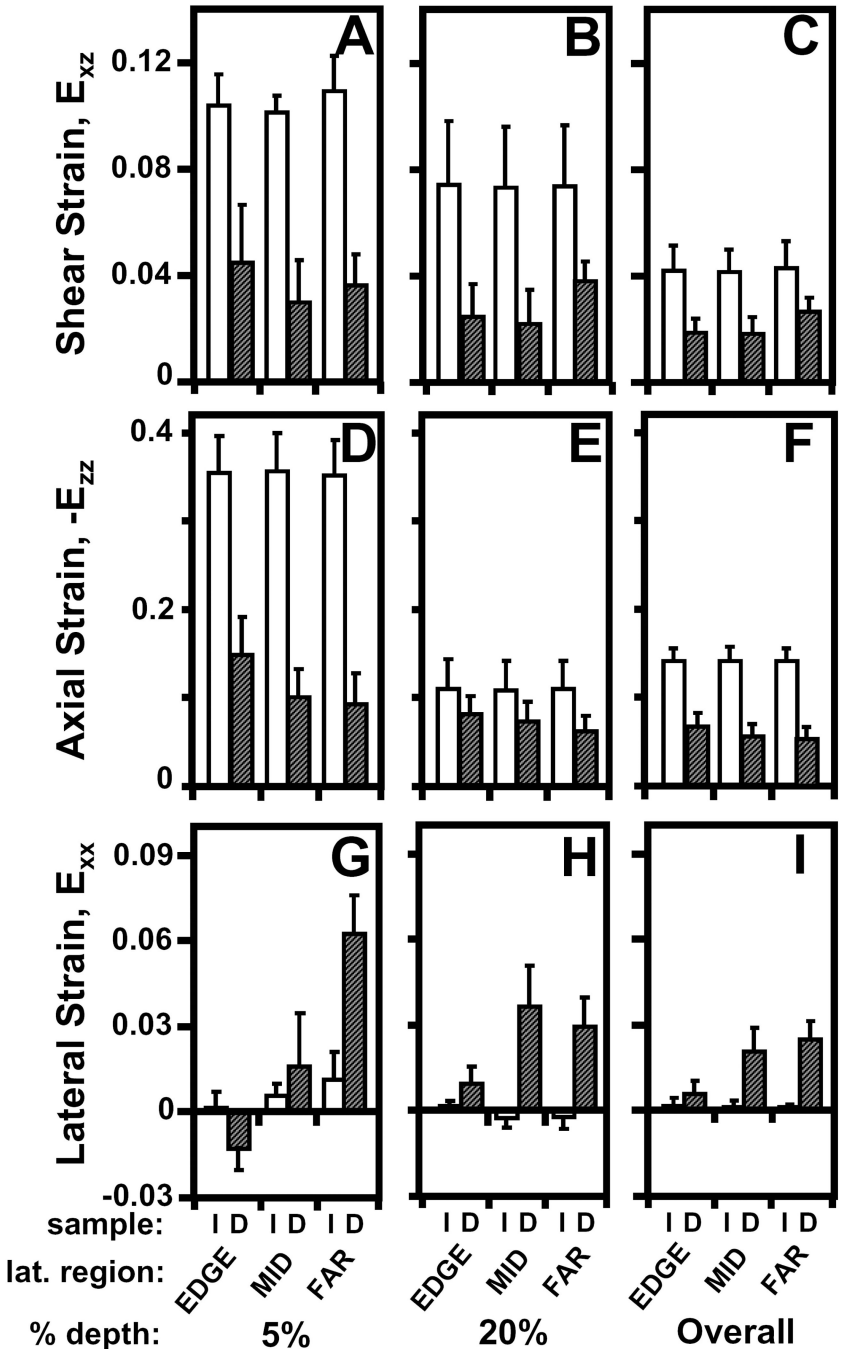

Figure 6.
Effect of a focal defect (intact (I) versus defect (D)) on (**A–C**) shear, (**D–F**) axial, and (**G–I**) lateral strain (**A,D,G**) near the articular surface, (**B,E,H**) at 20% tissue depth, and (**C,F,I**) overall of trochlear cartilage during articulation.

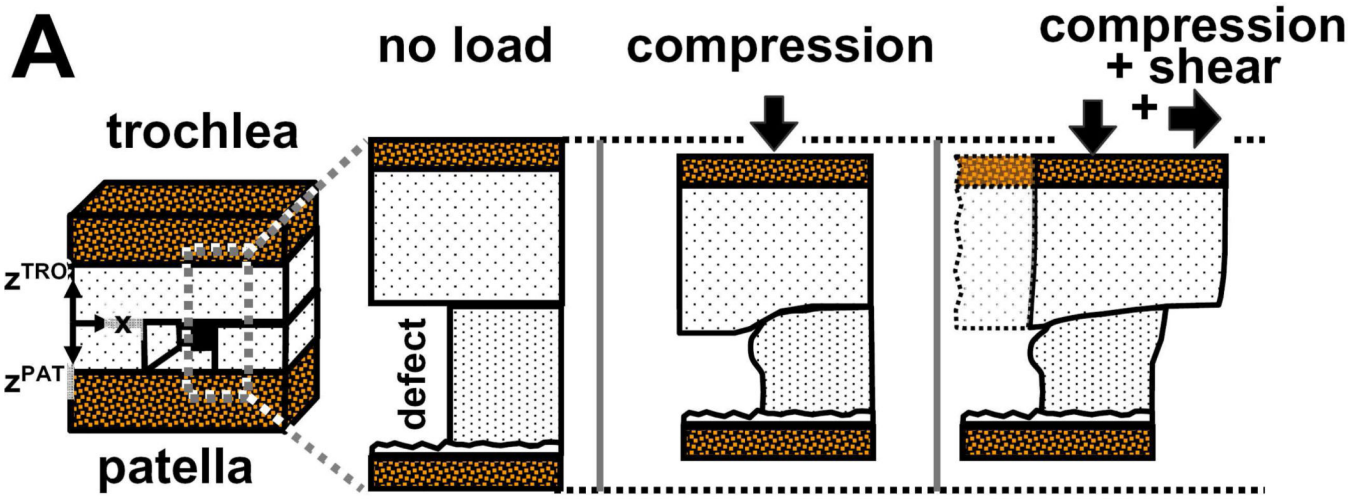

B

location	strain	relative changes in strain compared to intact		
trochlea	E_{xz}	—	↑↑	↓↓
	$-E_{zz}$	—	↓↓↓	↓↓
	E_{xx}	—	↑	↑↑
patella	E_{xz}	—	↑↑	↓↓/↑↑*
	$-E_{zz}$	—	↑	↑↑
	E_{xx}	—	—	↑↑↑

Figure 7.

(**A**) Schematic depicting the effect of a focal defect on tissue deformation of trochlear and patellar cartilage when unloaded, compressed, and compressed and sheared in apposition. (**B**) Table of relative changes in shear (E_{xz}), axial ($-E_{zz}$), and lateral (E_{xx}) strains compared to normal intact cartilage (i.e. without a focal defect) for both trochlear and patellar cartilage when they are unloaded, compressed, and compressed and sheared in apposition.